Atomic structure and transition properties of H-like Al in hot and dense plasmas*

Xiang-Fu Li(李向富)[1,2], Gang Jiang(蒋刚)[1,3,†], Hong-Bin Wang(王宏斌)[1], and Qian Sun(孙乾)[2]

[1] *Institute of Atomic and Molecular Physics, Sichuan University, Chengdu* 610065, *China*
[2] *College of Electrical Engineering, Longdong University, Qingyang* 745000, *China*
[3] *The Key Laboratory of High Energy Density Physics and Technology of Ministry of Education, Chengdu* 610065, *China*

(Received 13 July 2016; revised manuscript received 25 September 2016; published online 29 November 2016)

The atomic structure and transition properties of H-like Al embedded in hot and dense plasmas are investigated using modified GRASP2K code. The plasma screening effect on the nucleus is described using the self-consistent field ion sphere model. The effective nuclear potential decreases much more quickly with increasing average free electron density, but increases slightly with increasing electron temperature. The variations of the transition energies, transition probabilities, and oscillator strengths with the free electron density and electron temperature are the same as that of the effective nuclear potential. The results reported in this work agree well with other available theoretical results and are useful for plasma diagnostics.

Keywords: H-like Al, strongly-coupled plasmas, atomic structure, transition properties

PACS: 31.15.ac, 31.15.ag, 31.15.xr, 52.27.Gr **DOI:** 10.1088/1674-1056/26/1/013101

1. Introduction

The study of the structural properties of ions within various external environments, especially in hot and dense plasmas, became an important area of research many decades ago because of its potential applications in astrophysical systems, laser-produced plasmas, inertial confinement fusion, x-ray lasers, plasma spectroscopy, etc.[1–11] In addition, compared to free systems, many interesting phenomena have been observed in plasmas, particularly in strongly coupled plasmas (SCPs), such as energy level shifts, changes in line shape, broadening of spectral lines, ionization potential depression (IPD), changes in transition properties, and line merging.[12–16]

The intensity of the influence of the plasma on the tested ion can be measured using the coupling strength Γ, which is defined as the ratio of the average Coulomb energy between pairs of particles and their kinetic energy. $\Gamma < 1$ denotes weakly coupled plasmas (WCPs), which can be described by the standard Debye–Hückel model.[17] In early works, only the plasma screening effect on the nucleus–electron interaction was taken into account, for example, see Refs. [18]–[20] Recently, the plasma screening effect on the electron–electron interaction has also been included, as in the works of Li *et al.*[5] and Xie *et al.*[21] $\Gamma \geq 1$ refers to SCPs, which can be described by the ion sphere model (ISM).[22] The ISM assumes that free electrons in the ion sphere are distributed uniformly, but in actual plasmas, the distribution of free electrons is not homogeneous. Consequently, a better model, the self-consistent-field ion sphere model (SCFISM),[23] was proposed. It considers a self-consistent distribution between free electrons and bound electrons within the ion sphere, and the free electron distribution is described by the Boltzmann or Fermi–Dirac distribution function. In this work, the SCFISM is applied to describe the influence of strongly coupled plasmas on Al^{12+} ions.

The experimental observations[12,24–27] of Al explicitly demonstrated the effects of an SCP on the spectral properties. Saemann *et al.*[12] used a laser-produced plasma, which caused the laboratory plasma conditions to change rapidly, so local thermodynamic equilibrium was not maintained. Consequently, the experimental measurements became extremely complicated, leading to a loss of accuracy. Several remarkable improvements[24–27] have been made because Linac coherent light sources (LCLS) can create relatively long-lived high-density plasmas with homogeneous temperatures. Ciricosta *et al.*[26] found that the measured IPDs of highly charged Al were not consistent with the predictions of the most widely used theoretical model of Stewart and Pyatt (SP),[28] but in good agreement with the earlier model of Ecker and Kröll (EK).[29] However, this measurement was questioned in a subsequent theoretical study by Preston *et al.*,[29] who used both the SP and EK models for the spectral lines of H-like Al. ISM potentials were used in both the SP model and the EK model. Hoarty *et al.*[31,32] further observed the K-shell spectra of Al plasmas using the Orion laser device; the values of the IPDs were more consistent with the SP model than the EK model. This situation clearly requires extensive and accurate theoretical study of atomic structures for Al. The energy eigenval-

*Project supported by the National Natural Science Foundation of China (Grant Nos. 11474208 and 11565018), the Department of Education Fund Item of Gansu Province, China (Grant No. 2015B-109), and the Doctoral Scientific Fund Project of Longdong University, China (Grant No. XYBY1601).

†Corresponding author. E-mail: gjiang@scu.edu.cn

© 2017 Chinese Physical Society and IOP Publishing Ltd

ues of ns ($n = 1$, 2) and np ($n = 2$, 3) and the transition energies of the Lyman lines for Al^{12+} within the framework of the ISM were investigated by Bhattacharyya *et al.*[33,34] Das[35] investigated the variation of the transition energy with the free electron density of the 1s–2p transition for H-like Al using the ISM. Salzmann *et al.*[36] presented the variations of the atomic properties and the transition probabilities with the free electron density for the Al^{12+} ion.

GRASP2K[37,38] is a general-purpose relativistic atomic structure package. Many atomic structure and transition properties of neutral atoms or ions in a vacuum can be accurately calculated using this program, but these calculations cannot be performed for atoms or ions in external environments, such as plasma environments. To estimate the influence of hot and dense plasmas on the atomic structure and transition properties of H-like Al, we use both the ISM potential and the SCFISM potential instead of the original potential in the GRASP2K code to describe the plasma screening effect on the nucleus. Using the modified program, we estimate the effective nuclear potential and transition properties of the $1s(^2S_{1/2})$–$np(^2P_{3/2})$ ($n = 2$–4) transitions for H-like Al within SCP environments. The plasma parameters chosen in this paper are from 100 to 1000 eV for the electron temperatures and from 1.0×10^{21} to 3.3×10^{25} cm^{-3} for the average free electron densities.

2. Theoretical method

The SCFISM potential is added to the GRASP2K code to describe the screening effect of plasmas on the nucleus. The theory behind the SCFISM has already been discussed in the literature,[23,39,40] so it will only be introduced briefly here.

The SCFISM is based on the following principles: the atom is represented by a point-like nucleus with charge Z embedded at the center of a spherical cavity containing enough electrons to ensure global neutrality. The spherical cavity is called an ion sphere or Winger–Seitz sphere. The ion sphere radius R_0 is determined by the formula $4\pi R_0^3 n_f/3 = Z - N_b$, where n_f is the average free electron density and N_b is the number of bound electrons. The plasma is assumed to produce an electrically neutral background beyond the ion sphere radius R_0. Thus, the problem of atomic structure within dense plasmas depends on a self-consistent solution of the Dirac and Poisson equations related to bound electrons, free electrons, and charged particles in the ion sphere.

For an N-electron atom, the Dirac–Coulomb Hamiltonian containing all of the dominant interactions can be written as

$$H = \sum_{i=1}^{N} H_i + \sum_{i=1}^{N-1} \sum_{j=i+1}^{N} \frac{1}{r_{ij}}, \tag{1}$$

where the first term is the contribution from one body, and the second term in the sum is the interaction between bound electrons. H_i is defined as

$$H_i = c\boldsymbol{\alpha} \cdot \boldsymbol{p} + (\beta - 1)c^2 + U_i(r), \tag{2}$$

where the first and the second terms in Eq. (2) are the relativistic kinetic energy of a bound electron, and the last term is the effective nuclear potential experienced by this bound electron. We will discuss how to get U_i in the following paragraphs.

We begin with the Poisson equation for the potential experienced by a tested ion with nuclear charge Z. The total potential $\phi_{tot}(r)$, which is produced by nuclear charge Z, free electron density $n_f(r)$, bound electron density $n_b(r)$, and other plasma ions with density $n_i(r)$, satisfies the Poisson equation[39]

$$\nabla^2 \phi_{tot}(r) = -4\pi[Z\delta(r) + \bar{Z} n_i(r) - n_f(r) - n_b(r)]. \tag{3}$$

Other ions here are characterized by an average charge $\bar{Z}$. In the SCFISM, only one nucleus is located at the center of the ion sphere, and the perturbations from other ions are ignored in Eq. (3). The bound electron density $n_b(r)$ can be obtained in terms of the radial wavefunctions $P(r)$ and $Q(r)$, which are the large and small component radial wavefunctions, respectively. For a given bound state, $n_b(r)$ can be written as

$$n_b(r) = \sum_{i=1}^{M} q_i \frac{[P_i^2(r) + Q_i^2(r)]}{4\pi r^2}, \tag{4}$$

where q_i stands for the general occupation number of bound electrons in subshell i and M is the number of subshells. Equation (4) represents the spherically averaged bound electron density. We assume that free electrons in the ion sphere follow a Fermi–Dirac distribution in the plane wave momentum k space[40–44] and that the free electron density can be defined as

$$n_f(r) = \frac{1}{\pi^2} \int_{k_0(r)}^{\infty} \frac{k^2 \mathrm{d}k}{\mathrm{e}^{[\sqrt{k^2c^2 + c^4} - c^2 - \phi_{tot}(r) - \mu]/T} + 1}, \tag{5}$$

where $k_0(r) = [2\phi_{tot}(r)c^2 - \phi_{tot}^2(r)]^{1/2}$. The chemical potential μ is determined by

$$\int_0^{R_0} n_f(r) 4\pi r^2 \mathrm{d}r = Z - N_b, \tag{6}$$

with regard to the electrically neutral conditions supposed by the SCFISM. The boundary condition for the total potential is set as follows:

$$\phi_{tot}(r \geq R_0) = 0. \tag{7}$$

For $r < R_0$, the solution of the Poisson equation takes the form[39]

$$\phi_{tot}(r) = Z/r + \phi_f(r) + \phi_b(r), \tag{8}$$

which includes the contribution from the nucleus, free electrons, and bound electrons. The potential of the free electrons can be calculated by

$$\phi_f(r_i) = -4\pi \left[\frac{1}{r_i} \int_0^{r_i} n_f(r_1) {r_1}^2 \mathrm{d}r_1 + \int_{r_i}^{R_0} n_f(r_1) r_1 \mathrm{d}r_1 \right], \tag{9}$$

and the potential of the bound electrons is similar to that of the free electrons

$$\phi_{\rm b}(r_i) = -4\pi\left[\frac{1}{r_i}\int_0^{r_i} n_{\rm b}(r_1){r_1}^2\,{\rm d}r_1 + \int_{r_i}^{R_0} n_{\rm b}(r_1)r_1\,{\rm d}r_1\right]. \quad (10)$$

The effective nuclear potential is defined as

$$\phi_{\rm eff}(r) = Z/r + \phi_{\rm f}(r), \quad (11)$$

where $\phi_{\rm eff}(r)$ is equal to U_i in Eq. (2). To solve the bound electron wavefunctions in the framework of the SCFISM, the radial wavefunctions $P(r)$ and $Q(r)$ are assumed to satisfy the boundary condition and normalization condition

$$P(r) = 0, \quad Q(r) = 0, \quad (r \geq R_0), \quad (12)$$

$$\int_0^{R_0} [P^2(r) + Q^2(r)]\,{\rm d}r = 1. \quad (13)$$

If the electron temperature is so high that the kinetic energy completely overcomes the potential energy, equation (5) shows that the free electron density is spatially independent. This means that free electrons are uniformly distributed in the ion sphere. According to Eqs. (9) and (11), the effective nuclear potential can be reduced to the following uniform electron-gas model (UEGM):

$$\phi^{\rm UEGM}(r) = \frac{Z}{r} - \frac{Z - N_{\rm b}}{2R_0}\left[3 - \left(\frac{r}{R_0}\right)^2\right]. \quad (14)$$

This UEGM potential is the same as the ISM potential. However, the electron temperature in the actual plasma is finite, so the spatial distribution of free electrons is not uniform but similar to a Fermi–Dirac distribution. Once the contributions of the nuclear charge, bound electrons, and free electrons are included in the total Hamiltonian, the single-electron wavefunction can be obtained via the self-consistent-field method, which is carried out using the modified GRASP2K code.

In fact, our calculation has some deficiencies. First, the free electron exchange and correlation effects are neglected because they have only minor influences on the results.[45] Second, the neighboring-ion correlations are simply included by assuming an electrically neutral background outside of the sphere rather than using a pair correlation function. The method will be inadequate for very strongly coupled plasmas,[46] for example, a lattice-type structure builds up in the plasma. In this work, the ion–ion coupling parameter $\Gamma_{ii}(= Z^2/kTR_0) \leq 2$, and a homogeneous ion distribution outside the ion sphere is still a plausible approximation.

3. Results and discussion

3.1. Spatial distribution of free electrons

The spatial distributions of free electrons surrounding the H-like Al ion at one electron temperature and three free electron densities are shown in Fig. 1. As seen from the figure, there is a sharp increase in the spatial density of free electrons near the nucleus, while the distribution is almost homogeneous far away from the nucleus. This result indicates that the spatial variation of the free electron distribution in the ion sphere is dominated by the strong nuclear charge attraction, but the repulsions among electrons play a less important role. The figure also shows that the free electron density tends to extremely large values around the nucleus when the free electron density is very high. This is not a physical problem, but in the actual calculation, this singularity does not cause notable effects on the final results.

Figure 2 shows the spatial distributions of free electrons surrounding the H-like Al ion at an average free electron density $n_{\rm f} = 1.0 \times 10^{24}$ cm^{-3} and three electron temperatures $T_{\rm e} = 100$, 500, 1000 eV. It can be seen from Fig. 2(a) that the spatial distribution of free electrons decreases significantly around the nucleus with increasing electron temperature, and it becomes more homogeneous and approaches that of the ISM. Because the kinetic energies of free electrons increase with increasing electron temperature, the probability that free electrons are far from the nucleus is increased. That is, free electrons move more freely and tend to distribute uniformly.

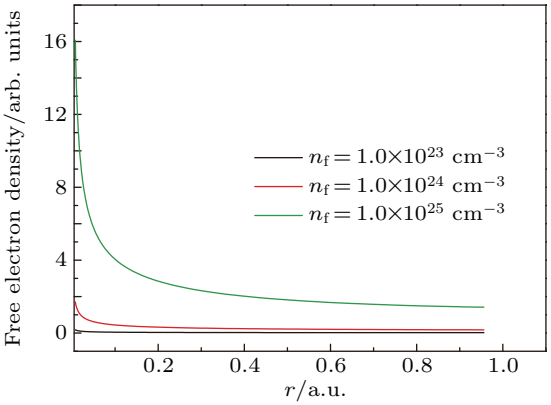


Fig. 1. (color online) Spatial distribution of free electrons surrounding the H-like Al ion at one electron temperature $T_{\rm e} = 500$ eV and three average free electron densities $n_{\rm f} = 1.0 \times 10^{23}$, 1.0×10^{24}, and 1.0×10^{25} cm^{-3}.

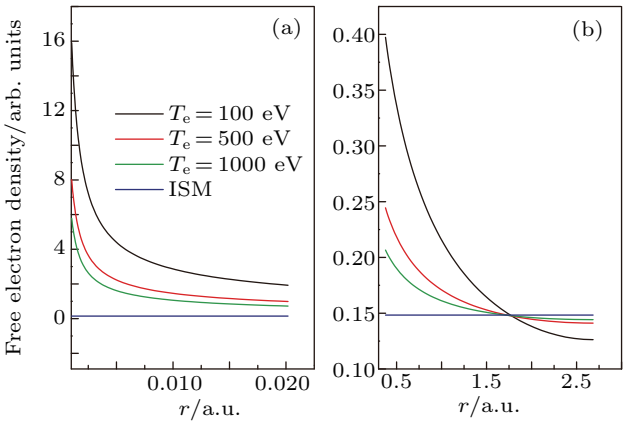


Fig. 2. (color online) (a) Spatial distribution of free electrons surrounding the H-like Al ion at one average free electron density $n_{\rm f} = 1.0 \times 10^{24}$ cm^{-3} and three electron temperatures $T_{\rm e} = 100$, 500, and 1000 eV, as well as that of ISM ($0 < r \leq 0.02$ a.u.); (b) the same as panel (a) ($0.25 < r \leq 2.7$ a.u.).

It is shown in Fig. 2(b) that the free electron density close to the surface of the ion sphere is lower than that of the ISM. This results from the electrical neutrality of the whole ion sphere. In other words, the number of electrons inside the ion sphere is equal to the nuclear charge Z.

As mentioned above, due to the strong nuclear charge attraction of highly charged ions, the spatial distribution of free electrons is not uniform except when the electron temperature is extremely high. Therefore, the SCFISM is more reasonable than the ISM for describing the plasma screening effect on the tested ion, although the free electron density close to the nucleus is too large to have any meaning at very high average free electron densities or very low electron temperatures.

3.2. Effective nuclear potential

The effective nuclear potentials $-rU_i$ of the H-like Al ion at four average free electron densities and one electron temperature are displayed in Fig. 3. The figure shows that the effective nuclear potential decreases with increasing r, and its minimum value is equal to the number of bound electrons. For the H-like Al ion, this value is 1.

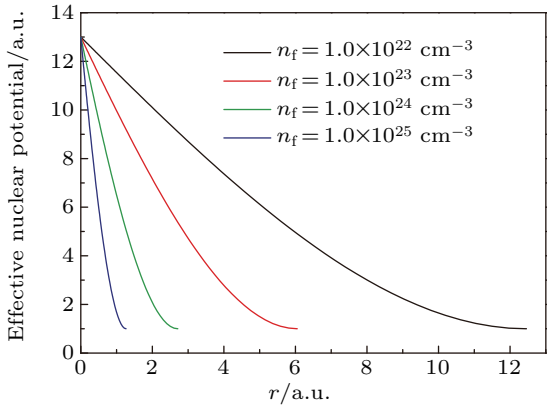


Fig. 3. (color online) Effective nuclear potential $-rU_i$ of the H-like Al ion at one electron temperature $T_e = 500$ eV and four average free electron densities $n_f = 1.0 \times 10^{22}$, 1.0×10^{23}, 1.0×10^{24}, and 1.0×10^{25} cm^{-3}.

It can also be seen from the figure that the effective nuclear potential decreases much more quickly as the average free electron density increases. Because the total electrical neutrality of the ion sphere is preserved, the radius of the ion sphere decreases with the increase in average free electron density. That is, more and more free electrons move around the nucleus as the average free electron density increases. The effective nuclear potential versus the average free electron density obtained in this work is similar to that of Be-like ions.[40]

The effective nuclear potentials $-rU_i$ of the H-like Al ion at two electron temperatures $T_e = 100$ and 1000 eV with an average free electron density $n_f = 1.0 \times 10^{24}$ cm^{-3} are shown in Fig. 4; the effective nuclear potential of the ISM is also plotted. The effective nuclear potential of the SCFISM approaches that of the ISM as the electron temperature increases because the spatial distribution of the free electrons becomes more homogeneous as the electron temperature increases. The other properties, such as the transition energies, transition probabilities, and oscillator strengths obtained by the SCFISM, also approach that of the ISM as the electron temperature increases. Therefore, in hot and dense plasmas, the screening effect of free electrons on the nucleus due to temperature is so important that it cannot be neglected.

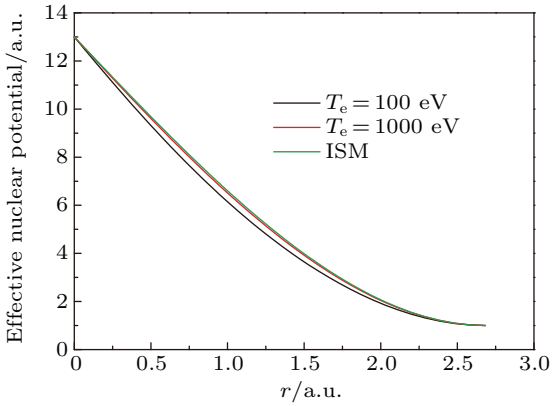


Fig. 4. (color online) Effective nuclear potential $-rU_i$ of the H-like Al ion at one average free electron density $n_f = 1.0 \times 10^{24}$ cm^{-3} and two electron temperatures $T_e = 100$ and 1000 eV, as well as that of ISM.

3.3. Transition properties of free H-like Al

Our calculations and NIST[47] both show that the energy level intervals between the $2p_{3/2}$ and $2p_{1/2}$, $3p_{3/2}$ and $3p_{1/2}$, and $4p_{3/2}$ and $4p_{1/2}$ atomic states are 1.301, 0.385, and 0.163 eV, respectively. The intervals of these energy levels are very small. The transition probabilities of $1s(^2S_{1/2})$–$np(^2P_{3/2})$ ($n = 2$–4) transitions are slightly larger than those of the corresponding $1s(^2S_{1/2})$–$np(^2P_{1/2})$ ($n = 2$–4) transitions. Therefore, only the transition properties of the $1s(^2S_{1/2})$–$np(^2P_{3/2})$ ($n = 2$–4) transitions are considered in this work. The electric dipole line strength S, transition probability A and oscillator strength gf in the length gauge is defined by[48]

$$S = \left[\langle \gamma_i J_i M_i | \sum_k^N r(k) | \gamma_j J_j M_j \rangle\right]^2, \tag{15}$$

$$Ag_j = 2.142 \times 10^{10} (E_{ij})^3 S, \tag{16}$$

$$gf = \frac{2}{3} E_{ij} S, \tag{17}$$

where $\langle \gamma_i J_i M_i | \sum_k^N r(k) | \gamma_j J_j M_j \rangle$ is the transition matrix element of transiting between atomic state i and atomic state j; E_{ij} is the transition energy (in a.u.) between the initial and final states with statistical weights g_i and g_j. The value of A is proportional to E_{ij}^3, the value of gf is proportional to E_{ij}, and they are all proportional to line strength S.

The transition energies, transition probabilities, and oscillator strengths of $1s(^2S_{1/2})$–$np(^2P_{3/2})$ ($n = 2$–4) transitions for the free H-like Al ion are displayed in Table 1, and the data collected by NIST[47] and the theoretical results of Jitrik *et al.*[49] are also listed. These data indicate that our results are in good agreement with NIST and Jitrik *et al.*

Table 1. The transition energies E (in eV), transition probabilities A (in s^{-1}), and oscillator strengths gf of $1s(^2S_{1/2})$–$np(^2P_{3/2})$ ($n = 2$–4) transitions for the free H-like Al ion. The values $x(y)$ indicate $x \times 10^y$.

Transition	E	E[47]	Dif1	A	A[49]	Dif2	gf	gf[49]	Dif3
1s–2p	1729.393	1728.989	0.02	1.787(13)	1.792(13)	0.28	0.551	0.553	0.36
1s–3p	2048.880	2048.469	0.02	4.775(12)	4.773(12)	0.04	0.105	0.105	0.0
1s–4p	2160.746	2160.332	0.02	1.947(12)	1.943(12)	0.21	0.038	0.038	0.0

3.4. Transition energies in plasmas

The transition energies of $1s(^2S_{1/2})$–$np(^2P_{3/2})$ ($n = 2$–4) transitions for the H-like Al ion in plasmas are displayed in Tables 2, 3, and 4, respectively. In addition, the results of the ISM are also listed. The change trends of the transition energies for $1s(^2S_{1/2})$–$np(^2P_{3/2})$ ($n = 2$, 4) transitions versus the average free electron density and electron temperature are the same as those of $1s(^2S_{1/2})$–$3p(^2P_{3/2})$ transition. Therefore, the $1s(^2S_{1/2})$–$3p(^2P_{3/2})$ transition is taken as an example to illustrate the influences of the free electron density and the electron temperature on the transition energies.

Table 2. Transition energies (in eV) of $1s(^2S_{1/2})$–$2p(^2P_{3/2})$ transition for the H-like Al ion in plasmas. The figures from 100 to 1000 are the electron temperatures (in eV). ISM is the result based on the ISM.

n_f/cm^{-3}	R_0/a.u.	100	200	300	400	500	600	700	800	900	1000	ISM
1.00(21)	26.8384	1729.387	1729.388	1729.389	1729.390	1729.390	1729.390	1729.390	1729.390	1729.390	1729.390	1729.391
2.21(21)	20.6048	1729.380	1729.382	1729.384	1729.385	1729.386	1729.386	1729.387	1729.387	1729.387	1729.387	1729.390
5.00(21)	15.6954	1729.365	1729.371	1729.374	1729.376	1729.378	1729.379	1729.380	1729.380	1729.381	1729.381	1729.386
1.00(22)	12.4573	1729.332	1729.350	1729.356	1729.359	1729.361	1729.363	1729.366	1729.366	1729.367	1729.369	1729.379
1.77(22)	10.2984	1729.288	1729.312	1729.323	1729.329	1729.334	1729.338	1729.341	1729.344	1729.346	1729.348	1729.369
5.00(22)	7.2851	1729.113	1729.179	1729.209	1729.230	1729.240	1729.247	1729.255	1729.260	1729.265	1729.268	1729.325
1.00(23)	5.7822	1728.861	1728.980	1729.039	1729.074	1729.095	1729.115	1729.125	1729.135	1729.145	1729.153	1729.258
1.42(23)	5.1444	1728.641	1728.813	1728.894	1728.942	1728.975	1728.999	1729.017	1729.032	1729.044	1729.055	1729.201
5.00(23)	3.3814	1726.954	1727.466	1727.742	1727.893	1727.996	1728.072	1728.131	1728.183	1728.226	1728.258	1728.717
6.56(23)	3.0888	1726.231	1726.916	1727.238	1727.435	1727.577	1727.676	1727.753	1727.814	1727.869	1727.911	1728.506
1.00(24)	2.6838	1724.683	1725.669	1726.154	1726.458	1726.658	1726.828	1726.928	1727.019	1727.099	1727.162	1728.039
2.21(24)	2.0604		1721.545	1722.496	1723.094	1723.521	1723.829	1724.068	1724.261	1724.420	1724.559	1726.386
5.00(24)	1.5695		1712.577	1714.430	1715.622	1716.476	1717.117	1717.628	1718.023	1718.365	1718.647	1722.501
1.00(25)	1.2457		1697.331	1700.493	1702.607	1704.131	1705.273	1706.187	1706.919	1707.536	1708.058	1715.258
1.77(25)	1.0298		1674.515	1679.114	1682.374	1684.764	1686.591	1688.073	1689.287	1690.299	1691.150	1703.184
2.43(25)	0.9266		1654.935	1660.564	1664.597	1667.635	1670.007	1671.939	1673.500	1674.822	1675.960	1692.028
3.00(25)	0.8637			1643.393	1648.141	1651.751	1654.604	1656.894	1658.785	1660.388	1661.768	1681.413
3.10(25)	0.8543				1645.139	1648.848	1651.685	1654.133	1656.094	1657.747	1659.159	1679.456
3.20(25)	0.8453						1648.886	1651.240	1653.356	1655.046	1656.493	1677.460
3.30(25)	0.8367								1650.567	1652.334	1653.814	1675.437

Table 3. Transition energies (in eV) of $1s(^2S_{1/2})$–$3p(^2P_{3/2})$ transition for the H-like Al ion in plasmas. The figures from 100 to 1000 are the electron temperatures (in eV). ISM is the result based on the ISM.

n_f/cm^{-3}	R_0/a.u.	100	200	300	400	500	600	700	800	900	1000	ISM
1.00(21)	26.8384	2048.854	2048.860	2048.863	2048.864	2048.866	2048.866	2048.867	2048.867	2048.868	2048.868	2048.872
2.21(21)	20.6048	2048.822	2048.834	2048.841	2048.845	2048.847	2048.849	2048.850	2048.851	2048.852	2048.853	2048.861
5.00(21)	15.6954	2048.750	2048.780	2048.793	2048.801	2048.807	2048.810	2048.813	2048.815	2048.817	2048.819	2048.836
1.00(22)	12.4573	2048.621	2048.681	2048.708	2048.721	2048.731	2048.738	2048.745	2048.749	2048.753	2048.757	2048.792
1.77(22)	10.2984	2048.427	2048.527	2048.571	2048.597	2048.615	2048.629	2048.639	2048.647	2048.654	2048.659	2048.724
5.00(22)	7.2851	2047.650	2047.916	2048.036	2048.108	2048.153	2048.186	2048.213	2048.233	2048.250	2048.263	2048.438
1.00(23)	5.7822	2046.492	2046.992	2047.226	2047.361	2047.449	2047.516	2047.562	2047.602	2047.635	2047.662	2047.994
1.42(23)	5.1444	2045.538	2046.229	2046.553	2046.738	2046.857	2046.948	2047.019	2047.077	2047.121	2047.159	2047.620
5.00(23)	3.3814	2037.923	2039.990	2040.980	2041.564	2041.960	2042.242	2042.463	2042.642	2042.785	2042.903	2044.382
6.56(23)	3.0888	2034.720	2037.358	2038.588	2039.335	2039.834	2040.203	2040.486	2040.710	2040.898	2041.046	2042.940
1.00(24)	2.6838	2027.797	2031.539	2033.326	2034.413	2035.144	2035.705	2036.098	2036.426	2036.695	2036.914	2039.688
2.21(24)	2.0604		2010.853	2014.368	2016.512	2017.998	2019.078	2019.918	2020.585	2021.128	2021.588	2027.266
3.00(24)	1.8609		1996.068	2000.664	2003.500	2005.457	2006.893	2008.007	2008.886	2009.612	2010.217	2017.774
3.20(24)	1.8213				2000.236	2002.301	2003.827	2005.009	2005.943	2006.749	2007.355	2015.378
3.31(24)	1.8008							2003.251	2004.220	2005.020	2005.682	2013.934

Table 4. Transition energies (in eV) of $1s(^2S_{1/2})$–$4p(^2P_{3/2})$ transition for the H-like Al ion in plasmas. The figures from 100 to 1000 are the electron temperatures (in eV). ISM is the result based on the ISM.

n_f/cm^{-3}	R_0/a.u.	100	200	300	400	500	600	700	800	900	1000	ISM
1.00(21)	26.8384	2160.675	2160.690	2160.697	2160.700	2160.703	2160.704	2160.706	2160.706	2160.708	2160.708	2160.716
2.21(21)	20.6048	2160.592	2160.622	2160.637	2160.645	2160.650	2160.654	2160.657	2160.659	2160.661	2160.663	2160.680
5.00(21)	15.6954	2160.403	2160.473	2160.503	2160.521	2160.533	2160.542	2160.548	2160.552	2160.557	2160.560	2160.597
1.00(22)	12.4573	2160.069	2160.207	2160.267	2160.299	2160.322	2160.337	2160.351	2160.359	2160.368	2160.375	2160.447
1.77(22)	10.2984	2159.565	2159.800	2159.900	2159.958	2159.997	2160.026	2160.047	2160.064	2160.077	2160.089	2160.217
5.00(22)	7.2851	2157.542	2158.144	2158.408	2158.565	2158.664	2158.736	2158.792	2158.835	2158.871	2158.899	2159.242
1.00(23)	5.7822	2154.528	2155.643	2156.138	2156.427	2156.617	2156.756	2156.857	2156.939	2157.007	2157.062	2157.709
1.42(23)	5.1444	2152.038	2153.557	2154.234	2154.630	2154.893	2155.082	2155.225	2155.338	2155.429	2155.505	2156.397
5.00(23)	3.3814	2130.551	2135.063	2137.045	2138.256	2139.068	2139.648	2140.098	2140.452	2140.820	2141.057	2143.837
6.00(23)	3.1821			2131.611	2133.041	2134.001	2134.699	2135.228	2135.640	2135.981	2136.264	2139.567
6.10(23)	3.1646				2132.506	2133.480	2134.173	2134.710	2135.133	2135.498	2135.787	2139.121
6.20(23)	3.1475						2133.657	2134.211	2134.620	2134.968	2135.259	2138.670
6.30(23)	3.1307									2134.456	2134.748	2138.213

Table 5. The highest free electron densities (in cm^{-3}) and the lowest electron temperatures (in eV) for which different spectral lines of the H-like Al ion can be observed. The notation $x(y)$ indicates $x \times 10^y$.

Spectral line	SCFISM[a]	ISM	Ref. [23]
Ly_α	3.1(25), 400; 3.2(25), 600; 3.3(25), 800	3.6(25)	3.52(25)
Ly_β	3.2(24), 400; 3.31(24), 700; 3.4(24), 1100	3.5(24)	3.31(24)
Ly_γ	6.0(23), 300; 6.1(23), 400; 6.2(23), 600; 6.3(23), 900	6.4(23)	

[a]In the results of SCFISM, the first number is the free electron density, and the second number is the electron temperature. For example, 3.1(25) is the free electron density, and 400 is the electron temperature.

Figure 5 shows the transition energies of $1s(^2S_{1/2})$–$3p(^2P_{3/2})$ transition for the H-like Al ion at different average free electron densities and one electron temperature $T_e = 500$ eV. It can be seen from the figure that the transition energies almost linearly decrease with increasing average free electron density because the screening effect of free electrons on the nucleus becomes stronger with increasing free electron density. For example, the transition energies obtained from the ISM are 2047.994, 2044.382, and 2039.688 eV at the average free electron densities of $n_f = 1.0 \times 10^{23}$, 5.0×10^{23}, and 1.0×10^{24} cm^{-3}, respectively. The results at these densities obtained by Bhattacharyya *et al.*[34] in the relativistic framework are 2047.985, 2044.336, and 2039.619 eV, respectively, which indicates that our results agree well with those of Bhattacharyya *et al.*

The transition energies of $1s(^2S_{1/2})$–$3p(^2P_{3/2})$ transition for the H-like Al ion at an average free electron density $n_f = 1.0 \times 10^{24}$ cm^{-3} and different electron temperatures are displayed in Fig. 6, and the result from the ISM is also included. The figure shows that the transition energies of the SCFISM increase and approach those of the ISM as the electron temperature increases because the higher the electron temperature, the more uniform the free electron distribution. Therefore, the screening effect of the free electrons on the nucleus becomes weaker, which leads to an increase in the transition energies.

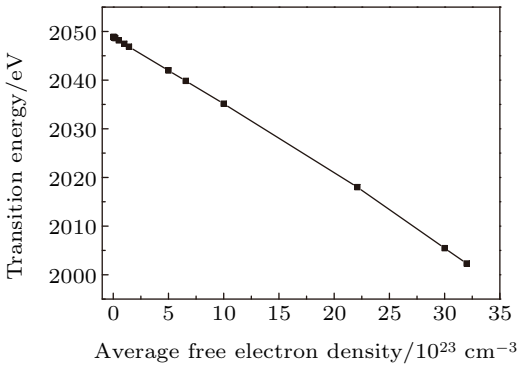


Fig. 5. Transition energies of $1s(^2S_{1/2})$–$3p(^2P_{3/2})$ transition for the H-like Al ion at different average free electron densities and one electron temperature $T_e = 500$ eV.

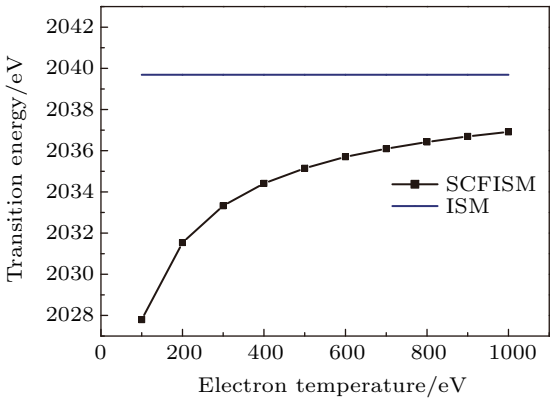


Fig. 6. Transition energies of $1s(^2S_{1/2})$–$3p(^2P_{3/2})$ transition for the H-like Al ion at an average free electron density $n_f = 1.0 \times 10^{24}$ cm^{-3} and different electron temperatures, as well as that of ISM.

3.5. Ionization potential depression

The ionization potentials (IPs) of $np_{3/2}$ [$n = 2$–4] atomic states for the H-like Al ion at one electron temperature $T_e = 900$ eV and different free electron densities are displayed in Fig. 7. As shown in the figure, for all atomic states, as the free electron density increases, the ionization potentials decrease and approach zero. If the IP is equal to zero at a given free electron density and electron temperature, the spectral line corresponding to that transition disappears because the electron in the higher orbital has been ionized. For example, the spectral line corresponding to $1s(^2S_{1/2})$–$4p(^2P_{3/2})$ transition disappears at the free electron density $n_f = 6.0 \times 10^{23}$ cm^{-3} and electron temperature $T_e = 300$ eV because the IP of $4p_{3/2}$ atomic state decreases to zero. Table 5 shows the highest free electron densities and the lowest electron temperatures for which different spectral lines of the H-like Al ion can be observed, and the results of Bhattacharyya *et al*.[33] are also listed. The data in the table indicate that our relativistic results based on the ISM agree well with the non-relativistic results based on the ISM of Bhattacharyya *et al*., and the highest free electron densities obtained from the SCFISM are smaller than those from the ISM. The results of the SCFISM may be more accurate than those from the ISM because the electron temperature is finite in actual plasmas, but the electron temperature is assumed to be ∞ in the ISM.

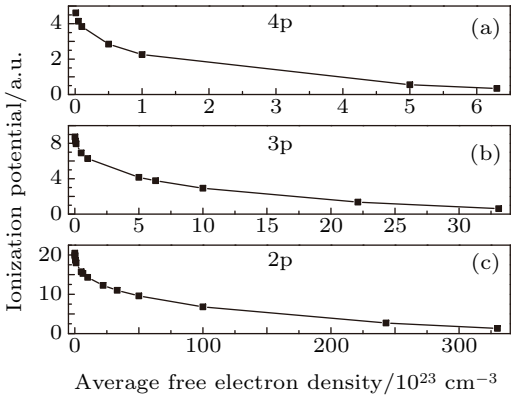


Fig. 7. Ionization potentials of (a) $4p_{3/2}$, (b) $3p_{3/2}$, (c) $2p_{3/2}$ atomic states for the H-like Al ion at one electron temperature $T_e = 900$ eV and different free electron densities.

3.6. Transition probabilities and oscillator strengths in plasmas

The transition probabilities and oscillator strengths of $1s(^2S_{1/2})$–$np(^2P_{3/2})$ ($n = 2$–4) transitions in the length gauge and velocity gauge are almost equal in our calculation, but the velocity results tend to be more sensitive to the accuracy of the wavefunctions than the length results. Therefore, only the results in the length gauge are presented in the appendix. The change trends of the transition probabilities and oscillator strengths versus the average free electron densities and electron temperatures are the same as that of the transition energies.

4. Conclusion

In this work, the atomic structure and transition properties of H-like Al embedded in hot and dense plasma environments are investigated. The SCFISM is better for describing the plasma screening effect on the nucleus than the ISM because the spatial distribution of free electrons is not uniform in actual plasmas except when the electron temperature is extremely high. There is a sharp increase in the spatial density of free electrons near the nucleus, while the distribution is almost homogeneous far from the nucleus. The spatial distribution of free electrons decreases significantly around the nucleus and becomes more homogeneous with increasing electron temperature. The effective nuclear potential decreases much more quickly as the average free electron density increases but only increases slightly as the electron temperature increases. The transition energies, transition probabilities, and oscillator strengths versus the free electron density and electron temperature are the same as the effective nuclear potential. The critical free electron densities above which different spectral lines disappear that are obtained using the SCFISM may be more accurate than those obtained using the ISM because the electron temperature is finite in actual plasmas, but the electron temperature is assumed to be ∞ in the ISM. The present SCFISM based on the GRASP2K code can be used to calculate relatively accurate atomic structure and transition properties for highly charged ions in SCP environments. The results reported in this work are useful for plasma diagnostics.

Acknowledgment

The authors express sincere gratitude to professor Jönsson P (Sweden) for providing the GRASP2K program freely. Xiang-Fu Li is grateful to professor Bhattacharyya S (India) for many useful discussions throughout the course of this work.

Appendix A

The transition probabilities and oscillator strengths of $1s(^2S_{1/2})$–$np(^2P_{3/2})$ ($n = 2$–4) transitions for H-like Al in the length gauge are listed in Tables A1–A6.

Table A1. Transition probabilities (in s^{-1}) of $1s(^2S_{1/2})$–$2p(^2P_{3/2})$ transition for the H-like Al ion in plasmas. The figures from 100 to 1000 are the electron temperatures (in eV). ISM is the result based on the ISM.

n_f/cm^{-3}	R_0/a.u.	100	200	300	400	500	600	700	800	900	1000	ISM
1.00(21)	26.8384	1.787(13)	1.787(13)	1.787(13)	1.787(13)	1.787(13)	1.787(13)	1.787(13)	1.787(13)	1.787(13)	1.787(13)	1.787(13)
2.21(21)	20.6048	1.786(13)	1.786(13)	1.787(13)	1.787(13)	1.787(13)	1.787(13)	1.787(13)	1.787(13)	1.787(13)	1.787(13)	1.787(13)
5.00(21)	15.6954	1.786(13)	1.786(13)	1.786(13)	1.786(13)	1.786(13)	1.786(13)	1.786(13)	1.786(13)	1.786(13)	1.786(13)	1.787(13)
1.00(22)	12.4573	1.786(13)	1.786(13)	1.786(13)	1.786(13)	1.786(13)	1.786(13)	1.786(13)	1.786(13)	1.786(13)	1.786(13)	1.786(13)
1.77(22)	10.2984	1.786(13)	1.786(13)	1.786(13)	1.786(13)	1.786(13)	1.786(13)	1.786(13)	1.786(13)	1.786(13)	1.786(13)	1.786(13)
5.00(22)	7.2851	1.785(13)	1.785(13)	1.785(13)	1.785(13)	1.786(13)	1.786(13)	1.786(13)	1.786(13)	1.786(13)	1.786(13)	1.786(13)
1.00(23)	5.7822	1.783(13)	1.784(13)	1.784(13)	1.784(13)	1.784(13)	1.785(13)	1.785(13)	1.785(13)	1.785(13)	1.785(13)	1.785(13)
1.42(23)	5.1444	1.781(13)	1.783(13)	1.783(13)	1.783(13)	1.784(13)	1.784(13)	1.784(13)	1.784(13)	1.784(13)	1.784(13)	1.785(13)
5.00(23)	3.3814	1.770(13)	1.773(13)	1.775(13)	1.776(13)	1.777(13)	1.777(13)	1.778(13)	1.778(13)	1.778(13)	1.778(13)	1.781(13)
6.56(23)	3.0888	1.765(13)	1.769(13)	1.772(13)	1.773(13)	1.774(13)	1.774(13)	1.775(13)	1.775(13)	1.776(13)	1.776(13)	1.779(13)
1.00(24)	2.6838	1.754(13)	1.761(13)	1.764(13)	1.766(13)	1.767(13)	1.768(13)	1.769(13)	1.770(13)	1.770(13)	1.770(13)	1.776(13)
2.21(24)	2.0604		1.732(13)	1.739(13)	1.742(13)	1.745(13)	1.747(13)	1.748(13)	1.750(13)	1.751(13)	1.752(13)	1.762(13)
5.00(24)	1.5695		1.670(13)	1.682(13)	1.689(13)	1.695(13)	1.699(13)	1.702(13)	1.704(13)	1.706(13)	1.708(13)	1.730(13)
1.00(25)	1.2457		1.563(13)	1.583(13)	1.596(13)	1.605(13)	1.612(13)	1.618(13)	1.622(13)	1.626(13)	1.629(13)	1.670(13)
1.77(25)	1.0298		1.414(13)	1.441(13)	1.460(13)	1.474(13)	1.485(13)	1.493(13)	1.500(13)	1.506(13)	1.511(13)	1.577(13)
2.43(25)	0.9266		1.300(13)	1.331(13)	1.353(13)	1.370(13)	1.383(13)	1.393(13)	1.402(13)	1.409(13)	1.415(13)	1.499(13)
3.00(25)	0.8637			1.256(13)	1.280(13)	1.299(13)	1.313(13)	1.325(13)	1.335(13)	1.343(13)	1.350(13)	1.447(13)
3.10(25)	0.8543				1.259(13)	1.278(13)	1.293(13)	1.305(13)	1.315(13)	1.324(13)	1.331(13)	1.431(13)
3.20(25)	0.8453						1.273(13)	1.285(13)	1.296(13)	1.304(13)	1.312(13)	1.415(13)
3.30(25)	0.8367								1.276(13)	1.285(13)	1.292(13)	1.398(13)

Table A2. Transition probabilities (in s^{-1}) of $1s(^2S_{1/2})$–$3p(^2P_{3/2})$ transition for the H-like Al ion in plasmas. The figures from 100 to 1000 are the electron temperatures (in eV). ISM is the result based on the ISM.

n_f/cm^{-3}	R_0/a.u.	100	200	300	400	500	600	700	800	900	1000	ISM
1.00(21)	26.8384	4.774(12)	4.774(12)	4.774(12)	4.774(12)	4.774(12)	4.774(12)	4.774(12)	4.774(12)	4.774(12)	4.774(12)	4.775(12)
2.21(21)	20.6048	4.773(12)	4.773(12)	4.774(12)	4.774(12)	4.774(12)	4.774(12)	4.774(12)	4.774(12)	4.774(12)	4.774(12)	4.774(12)
5.00(21)	15.6954	4.771(12)	4.772(12)	4.772(12)	4.772(12)	4.772(12)	4.772(12)	4.773(12)	4.773(12)	4.773(12)	4.773(12)	4.773(12)
1.00(22)	12.4573	4.767(12)	4.768(12)	4.769(12)	4.770(12)	4.770(12)	4.770(12)	4.770(12)	4.770(12)	4.770(12)	4.771(12)	4.771(12)
1.77(22)	10.2984	4.761(12)	4.764(12)	4.765(12)	4.766(12)	4.766(12)	4.766(12)	4.767(12)	4.767(12)	4.767(12)	4.767(12)	4.769(12)
5.00(22)	7.2851	4.737(12)	4.744(12)	4.747(12)	4.749(12)	4.751(12)	4.751(12)	4.752(12)	4.753(12)	4.753(12)	4.753(12)	4.758(12)
1.00(23)	5.7822	4.701(12)	4.715(12)	4.721(12)	4.724(12)	4.727(12)	4.729(12)	4.730(12)	4.731(12)	4.732(12)	4.732(12)	4.740(12)
1.42(23)	5.1444	4.671(12)	4.690(12)	4.699(12)	4.704(12)	4.707(12)	4.709(12)	4.711(12)	4.713(12)	4.714(12)	4.715(12)	4.725(12)
5.00(23)	3.3814	4.434(12)	4.489(12)	4.514(12)	4.529(12)	4.539(12)	4.546(12)	4.551(12)	4.555(12)	4.559(12)	4.562(12)	4.594(12)
6.56(23)	3.0888	4.332(12)	4.401(12)	4.433(12)	4.451(12)	4.464(12)	4.473(12)	4.479(12)	4.485(12)	4.489(12)	4.493(12)	4.534(12)
1.00(24)	2.6838	4.110(12)	4.207(12)	4.252(12)	4.278(12)	4.296(12)	4.309(12)	4.319(12)	4.326(12)	4.332(12)	4.338(12)	4.397(12)
2.21(24)	2.0604		3.521(12)	3.601(12)	3.650(12)	3.683(12)	3.707(12)	3.725(12)	3.739(12)	3.751(12)	3.761(12)	3.874(12)
3.00(24)	1.8609		3.123(12)	3.217(12)	3.275(12)	3.314(12)	3.342(12)	3.364(12)	3.382(12)	3.396(12)	3.407(12)	3.545(12)
3.20(24)	1.8213				3.362(12)	3.399(12)	3.427(12)	3.448(12)	3.464(12)	3.478(12)	3.489(12)	3.622(12)
3.31(24)	1.8008							3.383(12)	3.400(12)	3.414(12)	3.426(12)	3.562(12)

Table A3. Transition probabilities (in s^{-1}) of $1s(^2S_{1/2})$–$4p(^2P_{3/2})$ transition for the H-like Al ion in plasmas. The figures from 100 to 1000 are the electron temperatures (in eV). ISM is the result based on the ISM.

n_f/cm^{-3}	R_0/a.u.	100	200	300	400	500	600	700	800	900	1000	ISM
1.00(21)	26.8384	1.945(12)	1.946(12)	1.946(12)	1.946(12)	1.946(12)	1.946(12)	1.946(12)	1.946(12)	1.946(12)	1.946(12)	1.946(12)
2.21(21)	20.6048	1.943(12)	1.944(12)	1.944(12)	1.945(12)	1.945(12)	1.945(12)	1.945(12)	1.945(12)	1.945(12)	1.945(12)	1.945(12)
5.00(21)	15.6954	1.939(12)	1.941(12)	1.941(12)	1.942(12)	1.942(12)	1.942(12)	1.942(12)	1.942(12)	1.942(12)	1.942(12)	1.943(12)
1.00(22)	12.4573	1.932(12)	1.935(12)	1.936(12)	1.936(12)	1.937(12)	1.937(12)	1.937(12)	1.937(12)	1.937(12)	1.938(12)	1.939(12)
1.77(22)	10.2984	1.921(12)	1.925(12)	1.927(12)	1.928(12)	1.929(12)	1.929(12)	1.930(12)	1.930(12)	1.930(12)	1.930(12)	1.932(12)
5.00(22)	7.2851	1.876(12)	1.887(12)	1.892(12)	1.894(12)	1.896(12)	1.897(12)	1.898(12)	1.899(12)	1.899(12)	1.900(12)	1.905(12)
1.00(23)	5.7822	1.809(12)	1.828(12)	1.837(12)	1.841(12)	1.845(12)	1.847(12)	1.848(12)	1.850(12)	1.851(12)	1.852(12)	1.861(12)
1.42(23)	5.1444	1.752(12)	1.778(12)	1.789(12)	1.796(12)	1.800(12)	1.803(12)	1.805(12)	1.807(12)	1.808(12)	1.809(12)	1.822(12)
5.00(23)	3.3814	1.248(12)	1.314(12)	1.343(12)	1.361(12)	1.372(12)	1.380(12)	1.386(12)	1.390(12)	1.394(12)	1.397(12)	1.431(12)
6.00(23)	3.1821			1.281(12)	1.298(12)	1.309(12)	1.317(12)	1.323(12)	1.328(12)	1.332(12)	1.335(12)	1.370(12)
6.10(23)	3.1646				1.283(12)	1.294(12)	1.302(12)	1.308(12)	1.313(12)	1.317(12)	1.320(12)	1.356(12)
6.20(23)	3.1475						1.287(12)	1.293(12)	1.298(12)	1.302(12)	1.305(12)	1.341(12)
6.30(23)	3.1307									1.283(12)	1.290(12)	1.326(12)

Table A4. The oscillator strengths of $1s(^2S_{1/2})$–$2p(^2P_{3/2})$ transition for the H-like Al ion in plasmas. The figures from 100 to 1000 are the electron temperatures (in eV). ISM is the result based on the ISM.

n_f/cm^{-3}	R_0/a.u.	100	200	300	400	500	600	700	800	900	1000	ISM
1.00(21)	26.8384	0.551	0.551	0.551	0.551	0.551	0.551	0.551	0.551	0.551	0.551	0.551
2.21(21)	20.6048	0.551	0.551	0.551	0.551	0.551	0.277	0.551	0.551	0.551	0.551	0.551
5.00(21)	15.6954	0.551	0.551	0.551	0.551	0.551	0.551	0.551	0.551	0.551	0.551	0.551
1.00(22)	12.4573	0.551	0.551	0.551	0.551	0.551	0.551	0.551	0.551	0.551	0.551	0.551
1.77(22)	10.2984	0.551	0.551	0.551	0.551	0.551	0.551	0.551	0.551	0.551	0.551	0.551
5.00(22)	7.2851	0.550	0.550	0.550	0.550	0.550	0.550	0.550	0.550	0.550	0.550	0.551
1.00(23)	5.7822	0.550	0.550	0.550	0.550	0.550	0.550	0.550	0.550	0.550	0.550	0.550
1.42(23)	5.1444	0.550	0.550	0.550	0.550	0.550	0.550	0.550	0.550	0.550	0.550	0.550
5.00(23)	3.3814	0.547	0.548	0.548	0.548	0.549	0.549	0.549	0.549	0.549	0.549	0.549
6.56(23)	3.0888	0.546	0.547	0.547	0.548	0.548	0.548	0.548	0.548	0.548	0.548	0.549
1.00(24)	2.6838	0.544	0.545	0.546	0.546	0.546	0.547	0.547	0.547	0.547	0.547	0.548
2.21(24)	2.0604		0.539	0.540	0.541	0.542	0.542	0.542	0.542	0.543	0.543	0.545
5.00(24)	1.5695		0.525	0.527	0.529	0.530	0.531	0.532	0.532	0.533	0.533	0.538
1.00(25)	1.2457		0.500	0.505	0.508	0.510	0.511	0.512	0.513	0.514	0.515	0.523
1.77(25)	1.0298		0.465	0.471	0.476	0.479	0.481	0.483	0.485	0.486	0.487	0.501
2.43(25)	0.9266		0.437	0.445	0.450	0.454	0.457	0.459	0.461	0.463	0.464	0.483
3.00(25)	0.8637			0.429	0.434	0.439	0.442	0.445	0.447	0.449	0.451	0.472
3.10(25)	0.8543				0.429	0.433	0.437	0.440	0.442	0.444	0.446	0.468
3.20(25)	0.8453						0.432	0.435	0.437	0.439	0.441	0.464
3.30(25)	0.8367								0.432	0.434	0.435	0.459

Table A5. The oscillator strengths of $1s(^2S_{1/2})$–$3p(^2P_{3/2})$ transition for the H-like Al ion in plasmas. The figures from 100 to 1000 are the electron temperatures (in eV). ISM is the result based on the ISM.

n_f/cm^{-3}	R_0/a.u.	100	200	300	400	500	600	700	800	900	1000	ISM
1.00(21)	26.8384	0.105	0.105	0.105	0.105	0.105	0.105	0.105	0.105	0.105	0.105	0.105
2.21(21)	20.6048	0.105	0.105	0.105	0.105	0.105	0.105	0.105	0.105	0.105	0.105	0.105
5.00(21)	15.6954	0.105	0.105	0.105	0.105	0.105	0.105	0.105	0.105	0.105	0.105	0.105
1.00(22)	12.4573	0.105	0.105	0.105	0.105	0.105	0.105	0.105	0.105	0.105	0.105	0.105
1.77(22)	10.2984	0.105	0.105	0.105	0.105	0.105	0.105	0.105	0.105	0.105	0.105	0.105
5.00(22)	7.2851	0.104	0.104	0.104	0.104	0.104	0.104	0.104	0.104	0.104	0.104	0.105
1.00(23)	5.7822	0.103	0.104	0.104	0.104	0.104	0.104	0.104	0.104	0.104	0.104	0.104
1.42(23)	5.1444	0.103	0.103	0.103	0.104	0.104	0.104	0.104	0.104	0.104	0.104	0.104
5.00(23)	3.3814	0.098	0.099	0.100	0.100	0.100	0.100	0.101	0.101	0.101	0.101	0.101
6.56(23)	3.0888	0.096	0.098	0.098	0.049	0.099	0.099	0.099	0.099	0.099	0.099	0.100
1.00(24)	2.6838	0.092	0.094	0.095	0.095	0.096	0.096	0.096	0.096	0.096	0.096	0.097
2.21(24)	2.0604		0.080	0.082	0.083	0.083	0.084	0.084	0.084	0.085	0.085	0.087
3.00(24)	1.8609		0.072	0.074	0.075	0.076	0.076	0.077	0.077	0.078	0.078	0.080
3.20(24)	1.8213				0.077	0.078	0.079	0.079	0.079	0.080	0.080	0.082
3.31(24)	1.8008							0.078	0.078	0.078	0.078	0.081

Table A6. The oscillator strengths of $1s(^2S_{1/2})$–$4p(^2P_{3/2})$ transition for the H-like Al ion in plasmas. The figures from 100 to 1000 are the electron temperatures (in eV). ISM is the result based on the ISM.

n_f/cm^{-3}	R_0/a.u.	100	200	300	400	500	600	700	800	900	1000	ISM
1.00(21)	26.8384	0.038	0.038	0.038	0.038	0.038	0.038	0.038	0.038	0.038	0.038	0.038
2.21(21)	20.6048	0.038	0.038	0.038	0.038	0.038	0.038	0.038	0.038	0.038	0.038	0.038
5.00(21)	15.6954	0.038	0.038	0.038	0.038	0.038	0.038	0.038	0.038	0.038	0.038	0.038
1.00(22)	12.4573	0.038	0.038	0.038	0.038	0.038	0.038	0.038	0.038	0.038	0.038	0.038
1.77(22)	10.2984	0.038	0.038	0.038	0.038	0.038	0.038	0.038	0.038	0.038	0.038	0.038
5.00(22)	7.2851	0.037	0.037	0.037	0.037	0.038	0.038	0.038	0.038	0.038	0.038	0.038
1.00(23)	5.7822	0.036	0.036	0.036	0.018	0.037	0.037	0.037	0.037	0.037	0.037	0.037
1.42(23)	5.1444	0.035	0.035	0.036	0.036	0.036	0.036	0.036	0.036	0.036	0.036	0.036
5.00(23)	3.3814	0.025	0.027	0.027	0.027	0.028	0.028	0.028	0.028	0.028	0.028	0.029
6.00(23)	3.1821			0.026	0.026	0.026	0.027	0.027	0.027	0.027	0.027	0.028
6.10(23)	3.1646				0.026	0.026	0.026	0.026	0.027	0.027	0.027	0.027
6.20(23)	3.1475						0.026	0.026	0.026	0.026	0.026	0.027
6.30(23)	3.1307									0.026	0.026	0.027

References

[1] Gao C, Zeng J and Yuan J M 2011 *High Energy Density Phys.* **7** 54
[2] Killian T C, Pattard T, Pohl T and Rost J M 2007 *Phys. Rep.* **449** 77
[3] Saha B and Fritzsche S 2006 *Phys. Rev. E* **73** 036405
[4] Saha B, Mukherjee P K and Bielinska-Waz D 2005 *J. Quant. Spectrosc. Radiat. Transf.* **92** 1
[5] Li B W, Dong C Z, Jiang J and Wang J G 2010 *Plasma Science and Technology* **12** 372
[6] Winkler P 1996 *Phys. Rev. E* **53** 5517
[7] Griem H R 1988 *Phys. Rev. A* **15** 2943
[8] Skupski S 1980 *Phys. Rev. A* **21** 1316
[9] Rogers F J 1974 *Phys. Rev. A* **10** 2441
[10] Greig J R, Griem H R, Jones L A and Oda T 1970 *Phys. Rev. Lett.* **24** 3
[11] Dong C Z, Xie L Y, W J J and Jiang J 2005 *Chin. Phys.* **14** 1108
[12] Saemann A, Eidmann K, Golovkin I E, Mancini R C, Andersson E, Förster E and Witte K 1999 *Phys. Rev. Lett.* **82** 4843
[13] Gamelet G, Jacgle P, Lemaire P, Carrilon A 1990 *J. Quant. Spectrosc. Radiat. Transfer* **44** 71
[14] Böddeker S, Günter S, Könies A, Hitzschkeet L and Kunze H J 1990 *Phys. Rev. E* **47** 2785
[15] Bradley D K, Kilkenny J, Rose S J and Hares J D 1987 *Phys. Rev. Lett.* **59** 2995
[16] Nantel M, Ma G, Gu S, Côté C Y, Itatani J and Umstadter D 1998 *Phys. Rev. Lett.* **80** 4442
[17] Murillo M S and Weisheit J C 1998 *Phys. Rep.* **302** 1
[18] Saha B, Mukherjee P K, Bielińska-Waz D and Karwowskib J 2003 *J. Quant. Spectrosc. Radiat. Transfer* **78** 131
[19] Ray D and Mukherjee P K 1998 *J. Phys. B: At. Mol. Opt. Phys.* **31** 3479
[20] Ning L N and Qi Y Y 2012 *Chin. Phys. B* **21** 123201
[21] Xie L Y, Wang J G, Janev R K, Qu Y Z and Dong C Z 2012 *Eur. Phys. J. D* **66** 125
[22] Ichimaru S 1982 *Rev. Mod. Phys.* **54** 1017
[23] Rozsnyai B F 1972 *Phys. Rev. A* **5** 1137
[24] Vinko S M, Ciricosta O, Preston T R, *et al.* 2015 *Nature Commun.* **6** 6397
[25] Vinko S M, Ciricosta O, Cho B I, *et al*. 2012 *Nature* **482** 59
[26] Ciricosta O, Vinko S M, Chung H K, *et al*. 2012 *Phys. Rev. Lett.* **109** 065002
[27] Cho B I, Engelhorn K, Vinko S M, *et al*. 2012 *Phys. Rev. Lett.* **109** 245003
[28] Stewart J C, Pyatt K D 1966 *Astrophys. J.* **144** 1203
[29] Ecker G and Kroll W 1963 *Phys. Fluids* **6** 62
[30] Preston T R, Vinko S M, Ciricosta O, Chung H K, Lee R W and Warka J S 2013 *High Energy Density Physics* **9** 258
[31] Hoarty D J, Allan P, James S F, Brown C R D, Hobbs L M R, Hill M P, Harris J W O, Morton J, Brookes M G, Shepherd R, Dunn J, Chen H, Marley E V, Beiersdorfer P, Chung H K, Lee R W, Brown G and Emig J 2013 *Phys. Rev. Lett.* **110** 265003
[32] Hoarty D J, Allan P, James S F, Brown C R D, Hobbs L M R, Hill M P, Harris J W O, Morton J, Brookes M G, Shepherd R, Dunn J, Chen H, Marley E V, Beiersdorfer P, Chung H K, Lee R W, Brown G and Emig J 2013 *High Energy Density Physics* **9** 661
[33] Bhattacharyya S, Saha J K and Mukherjee T K 2015 *Phys. Rev. A* **91** 042515
[34] Bhattacharyya S, Sil A N, Fritzsche S and Mukherjee P K 2008 *Eur. Phys. J. D* **46** 1
[35] Das M 2012 *Physical of Plasmas* **19** 092707
[36] Salzmann D and Szichman H 1987 *Phys. Rev. A* **35** 807
[37] Jönsson P, He X H, Fischer C F and Grant I P 2007 *Computer Physics Communication* **177** 597
[38] Jönsson P, Gaigalas G, Bieron J, Fischer C F and Grant I P 2013 *Computer Physics Communication* **184** 2197
[39] Li X D, Xu Z Z and Rosmej F B 2006 *J. Phys. B: At. Mol. Opt. Phys.* **39** 3373
[40] Li Y Q, Wu J H, Hou Y and Yuan J M 2008 *J. Phys. B: At. Mol. Opt. Phys.* **41** 145002
[41] Rozsnyai B F 1982 *J. Quant. Spectrosc. Radiat. Transfer* **27** 211
[42] Rozsnyai B F 1991 *Phys. Rev. A* **43** 3035
[43] Liberman D A 1979 *Phys. Rev. A* **20** 4981
[44] Yuan J M 2002 *Phys. Rev. E* **66** 047401
[45] Skupsky S 1980 *Phys. Rev. A* **21** 1316
[46] Salzmann D, Yin R Y and Pratt R H 1985 *Phys. Rev. A* **6** 3627
[47] NIST Database
[48] Norrington P H, Kingston A E and Boone A W 2000 *J. Phys. B: At. Mol. Opt. Phys.* **33** 1767
[49] Jitrik O and Bunge C F 2004 *J. Phys. Chem. Ref. Data* **33** 1059